Intramolecular Reactions in Randomly End-Linked Polymer Networks and Linear (Co)polymerizations

Michael Lang,* Dietmar Göritz, and Stefan Kreitmeier

Institute of Experimental and Applied Physics, University of Regensburg, Polymer Physics, 93040 Regensburg, Germany

Received May 18, 2004; Revised Manuscript Received December 18, 2004

ABSTRACT: This work studies intramolecular reactions in irreversible linear and nonlinear random (co)polymerizations with computer simulations. We find a relative rate for the formation of rings of i chains proportional to $i^{-3/2}$ in agreement with predictions of rate theory based on Gaussian chain statistics. This result is used to develop a general ansatz for ring formation in irreversible random polymerizations or in cyclization equilibria. Using the approximation $c_{ext} \gg c_{int}$ for the concentrations of reactive groups on the external molecules c_{ext} and on the selected molecule c_{int}, this ansatz reduces to a result previously found by Suematsu. In this special case we find that the ring size distribution R_i is proportional $i^{-5/2}[(f - 1)(g - 1)p_A p_B]^{i-1}$, where f and g denote the functionality of two different types of molecules A and B, and p_A and p_B are the conversions of the reactive groups on the molecules, respectively. Our findings explain preceding experiments, simulations, and all results within this work as well as we can discuss the limitations of previous theoretical approaches.

1. Introduction

Theories of gelation or network structure[1−5] usually start with the simplifying assumption of no intramolecular reactions up to the gel point. However, it is known for many decades that this assumption is not true for any possible linear and nonlinear polymerizations: theories,[6−8] experiments,[9] and computer simulations[10−12] on cross-linked polymer networks show that approximately 20% or more of the cross-linking reactions yield inactive dangling loops, mostly depending on the chain statistics and the degree of dilution. For end-linking reactions this fraction is reported to range from 2% to 20% or sometimes more,[9,13−18] depending on the length of the polymer chains, the functionality of the cross-links, and the degree of dilution.

Since end-linked networks turned out to be useful for testing of theories of polymer networks,[19,20] they have been a frequent topic of theoretical works,[3,4,5,21,22] experiments,[20,23−25] and simulations[12−18] for the past decades. Since the analysis of cycle formation within linear polymerizations[26,28−32,34,43] is a useful tool to gain insight into the general characteristics of ring formation, we use this knowledge to combine it with theory on nonlinear polymerizations and polymer network formation.

In particular, we focus on random reactions and cyclization equilibria in order to develop a general approach for the theoretical description of this phenomenon, and simultaneously we test the results by computer simulations. To this end, we have to generalize the concepts for intramolecular reactions in linear and nonlinear reactions for systems that react at random or in cyclization equilibria. We retain two of Flory's[3] simplifying assumptions for polymer network formation: (a) all functional groups of the same type are equally reactive, and (b) all groups react independently of one another. In the remainder of this work we will abbreviate both assumptions by the term random reactions. The discussion of kinetically controlled reactions will be the topic of a succeeding work. Next we start with a brief summary of the theoretical fundamentals that are required to understand our computations.

For reversible reactions at thermodynamic equilibrium Jacobson and Stockmayer[26] developed the first ideas on ring formation. Their approach is based on the Gaussian distribution function Φ for the end-to-end vectors $\mathbf{R}$ of a random flight of N steps (i.e., the number of segments in a chain) of length b (the effective linking length between the monomers)[33]

$$\Phi(\mathbf{R},N) = \left(\frac{3}{2\pi N b^2}\right)^{3/2} \exp\left(-\frac{3\mathbf{R}^2}{2Nb^2}\right) \tag{1}$$

Combined with the change in conformational entropy, they found for the size distribution R_N of rings of N monomers the relationship

$$R_N \sim N^{-5/2} \tag{2}$$

This result was obtained by considering the fact that $|\mathbf{R}| \approx 0$ for ring formation implies for Gaussian chains

$$\Phi(0,N) \sim N^{-3/2} \tag{3}$$

Kloczkowski and Jernigan[26] showed recently that the probability for ring formation for short random flights in more detailed models is almost the same as in the classical work of Jacobson and Stockmayer. Only for short polymers additional effects have to be taken into account. Flory and co-workers[28,29,34] refined the work of Jacobson and Stockmayer using rotational isomeric models. They found that this refinement is essential for short rings which depend strongly on the specific molecular structure of the chains. However, for sufficiently long chains they only found a small shift to −2.55 for the exponent in eq 2. We concentrate in this work on the cases of ring chain equilibria or random reactions. Therefore, the above findings are important for our work because of (a) the Gaussian approximation is a good approximation for sufficiently long chains, (b)

* To whom correspondence should be addressed. e-mail michael1.lang@physik.uni-regensburg.de.

10.1021/ma049025z CCC: $30.25
Published on Web 02/09/2005

we need to estimate the density of the distribution function of the end-to-end vectors with $|\mathbf{R}| \approx 0$, and finally (c) the conditions of the reactions are important for the results.

The work of Jacobson and Stockmayer was often used in the literature for comparison with experiments. Semlyen,[33] for instance, summarizes a number of experiments concluding that this theory is a good approximation for most of the linear ring−chain equilibria. Only for short rings or some polar organic systems close agreement is not obtained.

For irreversible stepwise reactions Gordon and Temple[29] and later Stanford et al.[30,31] developed the main ideas. For a random alternating linear (difunctional) copolymer Gordon and Temple found

$$\frac{\mathrm{d}R_i}{\mathrm{d}t} \sim \frac{E_i}{(iN)^{3/2}} \tag{4}$$

where R_i denotes the number of rings made of i monomers of a minimum length N which is able to form a ring and E_i denotes the number fraction of chains of i monomer units. The exponent in the denominator results from the assumed Gaussian chain statistics analogue to eq 3. Because of eq 4, the formation of long cycles additionally depends on the distribution of E_i within the polymerizations, and thus, no general solution for this problem exists until now. However, in section 5 the solutions for the special cases of random reactions between the molecules or ring−chain equilibration reactions will be presented.

Stepto and co-workers[21,22,36−38] developed from the work of Kilb[39] an estimate for the gel point. To this end, ring forming parameters are calculated which determine the probability for intramolecular reactions assuming, that the chains are long enough to obey Gaussian statistics in good approximation. Let us consider the case of a random copolymerization of f-functional molecules of type A with g-functional molecules of type B. If $c_{\mathrm{A,int}}$ is the local intramolecular concentration of A groups around one selected reactive group B and $c_{\mathrm{A,ext}}$ is the concentration of A groups, that are not connected with B, an intramolecular reaction for B occurs with the probability

$$\lambda_{\mathrm{B}} = \frac{c_{\mathrm{A,int}}}{c_{\mathrm{A,int}} + c_{\mathrm{A,ext}}} \tag{5}$$

The probability λ_{A} and the concentrations $c_{\mathrm{B,ext}}$ and $c_{\mathrm{B,int}}$ are defined analogously. If p_{A} and p_{B} are the overall extents of reaction of A and B groups, respectively, and c_{A0} and c_{B0} are the concentrations of the groups at the beginning of the reaction, it directly follows $c_{\mathrm{A,ext}} = c_{\mathrm{A0}}(1 - p_{\mathrm{A}})$ and $c_{\mathrm{B,ext}} = c_{\mathrm{B0}}(1 - p_{\mathrm{B}})$. Using eq 3 and the approximation $c_{\mathrm{ext}} \gg c_{\mathrm{int}}$, the relative dependence

$$P_i = P_1 i^{-3/2} \tag{6}$$

for the probability P_i of rings of i chains with Ni monomers is obtained. In this approach and in the following we use the length N as the number of skeletal bonds between equivalent points in the structure, e.g., the branching point of one type of molecule. Equation 6 is used to calculate $c_{\mathrm{A,int}}$ and $c_{\mathrm{B,int}}$ via

$$c_{\mathrm{int}} = \sum_i c_{\mathrm{int},i} = \sum_i n_i P_i \tag{7}$$

where n_i is the number of the possible intramolecular pairs of length Ni. Assuming a linear sequence for the summation $n_i = 1$ for all i in eq 7 the condition for gelation is obtained from the Flory result

$$p_{\mathrm{A_c}}(f - 1)p_{\mathrm{B_c}}(g - 1) = 1 \tag{8}$$

by multiplying with the fraction of the respective intermolecular reactions as defined by eq 5. This leads to

$$p_{\mathrm{A_c}}(1 - \lambda_{\mathrm{B}})(f - 1)p_{\mathrm{B_c}}(1 - \lambda_{\mathrm{A}})(g - 1) = 1 \tag{9}$$

Here $p_{\mathrm{A_c}}$ and $p_{\mathrm{B_c}}$ denote the conversion of the groups at the critical point. Note that the choice of the above linear sequence for calculation was motivated by the good agreement between theory and experiments in this case.

Leung and Eichinger[13,14] have been the first to investigate cycle formation with computer simulations of networks. Since their calculations are motivated by their simulation method, we have to make some remarks on this method. They use a static approach based on phantom chains with Gaussian statistics for the analysis of end-linking reactions. At the beginning of the simulation a start configuration of polymers and cross-links is generated. Within a given cutoff distance d possible partners for reaction were selected and reordered concerning their pairwise distances. Beginning with the smallest distances, the reactions are assigned to the reactive monomers and the reaction is driven to completion by a stepwise increase of d. Thus, for this simulation method, the reactions depend on the pairwise distribution of particles in space. They found the following empirical relation for rings of one chain

$$R_1 = k'(f - 1)N^{-3/8} \tag{10}$$

k' is a factor that was observed to be roughly proportional to the extent of reaction, f denotes the functionality of the cross-links, and N counts the number of repeat units in the polymer chains. Motivated by their simulations, where a capture radius determined the partners for reaction, they derived the equation

$$P_1(N) = k''N^{-0.406} \tag{11}$$

for the probability $P_1(N)$ of loop formation as a function of the initial chain length N by consideration of the statistical distribution of nearest neighbors with random positions. However, both simulation and theory are based on the same static approach without any motion of the molecules disregarding the self-avoidance of the chains and using a somewhat artificial linking procedure. This may have an effect on the results.

Suematsu[40,41] separates intermolecular reactions from reactions that lead to ring formation. In particular, at the gel point p_{c} it follows

$$p_{\mathrm{c}} = p_{\mathrm{inter}} + p_{\mathrm{ring}} \tag{12}$$

which is in principle the same idea as in eqs 5 and 9. For the general case of a random copolymerization of M_0 f-functional units of type A and N_0 g-functional B units p_{ring} can be written as

$$p_{\mathrm{ring}} = \Gamma/gM_0$$

with the number of rings Γ at the gel point. Using the

ideal gel point from Flory[2] for p_{inter} and restricting to the equimolar case, eq 12 can be rewritten as

$$p_c = \frac{1}{[(f_e^* - 1)(g_e^* - 1)]^{1/2}} + \frac{(f+g)[\Gamma]}{fg}\gamma \quad (13)$$

where f_e^* and g_e^* denote the effective intermolecular functionalities, $[\Gamma] = \Gamma/V$ is the number concentration of rings at the gel point, and $\gamma = V/(M_0 + N_0)$ is the reciprocal of the initial concentration of the monomers. Suematsu argues[40] that in the limit of high concentrations of polymers $\gamma \to 0$ an asymptotic solution for the ring concentration $[\Gamma]$ in eq 13 results from the probability of i-ring formation

$$P_i \sim \gamma\varphi_i[(f-1)(g-1)p_A p_B]^{i-1} \quad (14)$$

by integration regarding the extent of reaction to

$$[\Gamma]_{\gamma=0} = \sum_{i=1}^{\infty}\varphi_i[(f-1)(g-1)p_A p_B]^i/2i \quad (15)$$

φ_i denotes the relative frequency of intra- to intermolecular reactions in a chain of i monomers. In effect, this limit $\gamma \to 0$ has to be understood similar to $c_{ext} \gg c_{int}$ because in the true limit $\gamma \to 0$ ring formation is not possible. The term in the square brackets of the above equations results from considering the expected number of chances for ring formation. Using Gaussian chain statistics, φ_i is expected to be proportional to $i^{-3/2}$ in the above limit $\gamma \to 0$. Note that eq 15 is physically meaningful only below the gel point due to the infinite summation. At the gel point the asymptotic solution for $\gamma \to 0$ reduces to $[\Gamma] = \sum_i \varphi_i/2i$, and thus

$$[\Gamma_i] \sim i^{-5/2} \quad (16)$$

because of $(f-1)(g-1)p_A p_B \to 1$.

Altogether, the preceding work seems to be contradictory when looking e.g. at the exponents for rings of i chains. Additionally, it is not clear how far the different assumptions affect the results of the calculations. Therefore, a test for these theories by computer simulations should be very interesting. Note that in our simulations and the discussion below we always will discuss molecular species that are able to form rings within the smallest linear unit, as each of the above theories assumes.

2. Simulation Method

We summarize briefly the basics of the simulation method which was developed by Carmesin and Kremer[42] as far as it is required for understanding our discussions. The monomers of these simulations are represented by cubes occupying eight adjacent sites on a cubic lattice (cf. Figure 1). The segments connecting the monomers are incorporated by a set of 108 possible bond vectors, which ensure that self-avoidance of the monomers implies a cut-avoidance of the bonds, while permitting maximum flexibility. The dynamics are obtained by random jumps of a monomer by one lattice unit. Since we are only interested in general structural aspects, we chose an athermal algorithm without van der Waals interaction in order to save computing time. The system was confined in a box with impenetrable walls. The size of the box was chosen in order to define the occupation density of the lattice (cf. Table 1) at a given number of monomers. No periodic boundary conditions were applied in order to facilitate simulations of swelling and deformation behavior as described in refs 43 and 44. Both kinds of simulation, based on the networks of this study, will be the topic of a subsequent work.

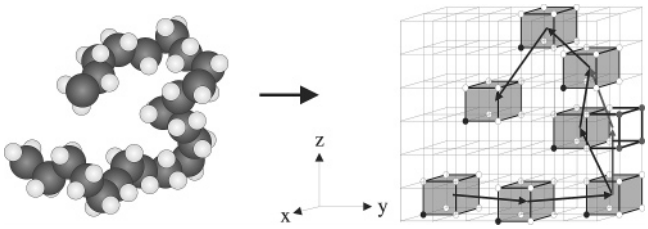

Figure 1. Visualization of the representation of a short polymer chain (left side) in the bond fluctuation method (right side): the fourth monomer (gray cube) of the chain in the simulation performs a random jump to the right of one lattice unit. The arrows indicate the bonds between the monomers.

Table 1. Parameters of the Simulations: Densities and Lattice Sizes[a]

	100% polymer		50% polymer	
N	monomer density	lattice size	monomer density	lattice size
10	61.2%	104^3	32.8%	128^3
22	58.6%	136^3	31.1%	168^3
43	60.1%	168^3	31.7%	208^3
82	60.1%	208^3	32.2%	256^3
153	60.0%	256^3	30.7%	320^3

[a] N denotes the length of the 8192 unimodal chains for each system. The monomer density on the particular simulation lattice was calculated for the $f = 4$ case and depends slightly on the functionality. The "100% polymer" case corresponds to systems with 100% volume content of polymer and the 50% case to a volume content of 50% polymer as explained in the text.

The polymer chains were obtained by a chain polymerizations process starting with a certain number of seed monomers and successively adding monomers until the desired length N was reached. After relaxation to equilibrium, the cross-links were inserted and curing was performed. The curing process was implemented in the same manner as in the simulations of Trautenberg et al.:[17] whenever a chain monomer reaches one of the six nearest-neighbor positions of a cross-link or vice versa, the two monomers were connected by a bond. More technical details on the simulation method and the implementation of the end-linking process are described elsewhere.[17,42,45,46] However, for our work it is important to note that this is a dynamic simulation of cut-avoiding chains built by self-avoiding monomers and that reactions take only place, when two monomers meat each other by diffusion.

It is obvious that the underlying lattice of this simulation method influences the results on short time and length scales. However, we want to analyze the stepwise polymerizations of long chains and the formation of polymer networks. Both happen on simulation times and length scales which clearly cannot be affected by the underlying lattice of these simulations. In addition, we have to remark that a bond of this simulation method corresponds to three or more atomic bonds in the backbone of a real polymer chain. This has to be considered when comparing our simulations with real polymer systems. Details on length and time scales for this kind of simulations and how this simulation method

can be compared with real polymers or other simulation methods can be found in ref 47.

3. Simulated Systems

For our investigations we generated 10 different melts, each made of 8192 unimodal chains, i.e., chains of identical length. We used the lengths $N = 10$, 22, 43, 82, and 153 monomers for the polymer chains and created systems at approximately 60% and 30% occupation density of the lattice which correspond approximately to 100% polymer and 50% polymer in the reaction container (cf. Table 1 for the densities and lattice sizes). To investigate the effect of the functionality of the cross-links on cycle formation, we inserted the stoichiometric numbers of 8192, 5461, 4096, 3277, and 2731 cross-links for the functionalities of $f = 2$, 3, 4, 5, and 6 at random positions. Because of limitations in computing time, we only generated additionally nine other statistically independent systems for the most interesting case of $f = 4$ and four other statistically independent systems for $f = 2$ for each chain length and both densities, respectively.

To estimate the effect of the borders, we compared the results for the innermost 50% of the systems with the whole system. Since the gel point is reached very quickly and thus for $f \geq 3$ the mean positions of the chains become located very fast, it was sufficient to analyze the distance to the border at the end of the simulations and not during cross-linking. In case of $f = 2$ we compared the data for the complete systems with the equivalent networks obtained for $f = 4$, where we were able to distinguish between the border and the innermost 50%. Note that the systems can be compared directly concerning properties which are based on the statistics of the chains, since the underlying polymer melts were identical except of the inserted cross-links.

Leung and Eichinger[13,14] found by comparison of systems with different size that there are almost no changes in network structure due to the finite size of the sample, if the system consists of more than 5000 chains. This is an important point because the size distribution of the cyclic structures should not be an artifact of the small number of chains in the simulation container. Each systems of this work consists of 8192 chains and is above this limit. However, the estimate of Leung and Eichinger is valid for full conversion, but at the gel point the required length scale for simulation grows to infinity. Thus, we perform a separate analysis of the cyclic structures close to the estimated critical point, where we expect the clearest influence of finite size.

In a network there is always a huge number of rings that can be constructed starting with an active network chain. According to this we restricted our analysis to the smallest ring possible. In the present work we used an algorithm[50] specialized for the detection of a spanning set of minimal cyclic structures representing the polymer network. This approach allows us to use the same method for analysis before and beyond the gel point.

4. Results of the Simulations

In this section we summarize the results of the simulations. The discussion of the data and the comparison with theory follow in the next section. In our simulations cross-links only react with chain ends. Thus, we can simulate a stepwise irreversible copolymerization of difunctional chains of N monomers with monomeric cross-links. The polymerizations was stopped when recognizing a drastic slowdown in the reaction speed. This point was between 98% and 99.2% extent of reaction for the linear polymerizations, which are discussed in the following.

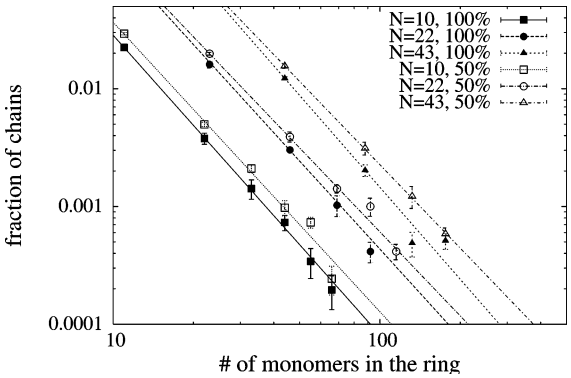

Figure 2. Number of rings of i chains normalized to the number of chains in the system represented as a function of the number of monomers N within the rings. N is the number of monomers between the junctions. The full symbols show the results for the systems with 100% volume content of polymer and the hollow symbols the results for the systems with 50% volume content of polymer.

Table 2. Fitting Parameters for the *i*-Ring Distributions in Linear Polymerizations[a]

N	density	a	b
10	50% polymer	11 ± 2	-2.46 ± 0.07
22	50% polymer	34 ± 6	-2.37 ± 0.05
43	50% polymer	115 ± 8	-2.35 ± 0.02
10	100% polymer	10.0 ± 0.9	-2.55 ± 0.04
22	100% polymer	41 ± 16	-2.5 ± 0.1
43	100% polymer	230 ± 180	-2.6 ± 0.2

[a] This table shows the parameters for the functions $h(N) = a(N)^b$ used to fit the mutual dependence of rings of i chains as displayed in Figure 2.

First, we analyze the number fraction of rings made of i chains. Figure 2 shows the average results for the samples with $N = 10$, 22, and 43 monomers and $f = 2$. Note that the number of rings is normalized to the number of chains at the beginning of the reaction for each of our figures and tables. In addition, we have to note that the length of the cyclic structures is equal to $N + 1$ since we have to take the cross-links into account. Because of the small number of rings for $f = 2$, we apply this analysis to the systems with $N \leq 43$ only. Table 2 shows the results for a least-squares fit for a function of type $h(iN) = a(iN)^b$ for each of the six series of investigated systems. The indicated error was calculated from the scatter of the data points by the fitting routine in order to test whether a function of this type can be used to describe the data. The results clearly show that the exponent b is in the range of $-5/2$. However, the statistical errors of the data in Figure 2 and the low ring fraction indicate that larger systems are needed for $f = 2$ in order to determine a more exact value for a. Nevertheless, the trend for the exponent b is clear.

Next, we analyze the development of the number of ring molecules of a specific size during the reaction for the above systems. Since we want to apply the mathematics of random reactions according to the ideas of Flory, we have to test the statistical independence of the reactions in our simulations. If we assume random reactions, the distribution of reacted groups on the

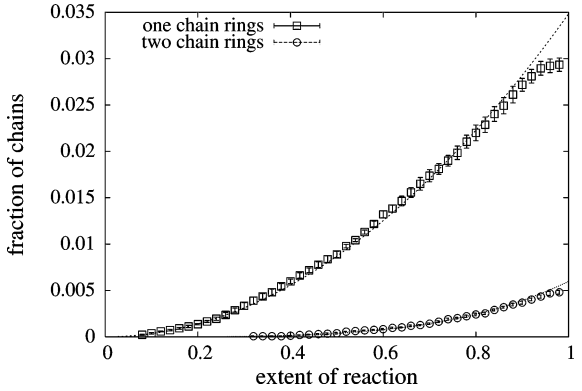

Figure 3. Number of one chain and two chain rings is normalized to the number of chains in the system and displayed as a function of the extent of reaction. The averages over five independent linear polymerizations with $N = 10$ at 50% volume content of polymer are shown. The lines show the fitting of the data with functions of type $h_i(p) = a_i p^{2i}$.

Table 3. One- and Two-Chain Rings in Linear Polymerizations[a]

N	density	$a_1[10^{-4}]$	$a_2[10^{-4}]$	$a_1/2a_2$
10	50% polymer	349 ± 4	60 ± 2	2.9
22	50% polymer	215 ± 2	44 ± 1	2.4
43	50% polymer	168 ± 1	39 ± 4	2.2
10	100% polymer	264 ± 5	47 ± 1	2.8
22	100% polymer	200 ± 5	34 ± 1	2.9
43	100% polymer	143 ± 2	21 ± 1	3.4

[a] This table summarizes the parameters for the functions $h_i(p) = a_i p^{2i}$ with $i = 1, 2$ used for the analysis of plots equivalent to Figure 3.

molecules is a function of conversion only. Therefore, we should find for each type of molecules (chains or cross-links) in our systems: (a) for the fraction of molecules with two bonds ap^2, (b) for the fraction with one bond reacted $b2p(1 - p)$, (c) for the unreacted part the fraction $c(1 - p)^2$, and in each case $a = b = c = 1$. As an example we present the data for a least-squares fit of the "worst case" with $N = 10$ at 30% lattice occupation density. For the chains we obtained $a = 1.010 \pm 0.004$, $b = 0.975 \pm 0.002$, and $c = 1.004 \pm 0.001$, and for the cross-links $a = 1.014 \pm 0.001$, $b = 0.962 \pm 0.002$, and $c = 1.005 \pm 0.001$. Thus, we can use the assumption of statistically independent reactions for the description of our simulations in good approximation.

Figure 3 shows the average number of rings made of one or two chains for the five systems with $N = 10$% and 50% polymers. We found very good agreement with functions of type $h_i(p) = a_i p^{2i}$ for a ring of i-chains using $a_1 = 0.0697 \pm 0.0005$ and $a_2 = 0.0120 \pm 0.0002$ when using the data for $p \leq 0.75$. The lines display these fitting functions. Table 3 summarizes the analogous results for all investigated systems with $f = 2$. The origin of the deviations at the end of the reaction is explained below in more detail. For the following discussion we identify the extrapolated value $R_1^* = a_1$ for the one chain rings at $p \rightarrow 1$ as key parameter for all systems.

For the nonlinear polymerizations the reaction stopped between 94% (for the systems with long chains or high functional cross-links) and 98% extent of reaction. Since we recorded the reactions during the formation of the networks, we are able to trace back to any point in this process. Thus, for the following analysis we compare all systems at 94% conversion in order to avoid additional influences of different conversions.

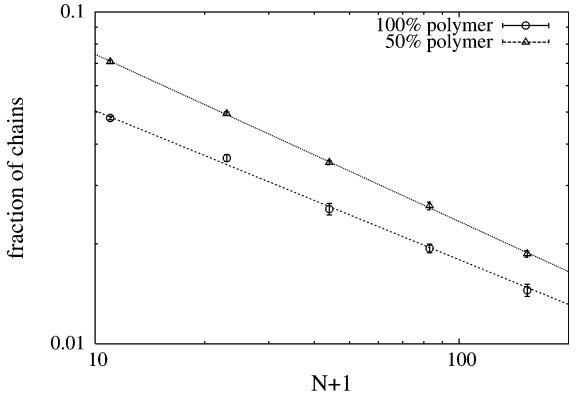

Figure 4. Number of one chain rings normalized to the number of chains for the innermost 50% of the sample. The data points are averaged over 10 independent networks with $f = 4$ and displayed for systems with 100% and 50% volume content of polymer in the reaction container.

Figure 4 shows the fraction of one chain rings in case of $f = 4$. We used a function of type $h(iN) = a(iN)^b$ for fitting the data of the systems with $f = 2$ and $f = 4$ and present the results in Table 4. The indicated error was calculated from the scatter of the data points. The difference at $f = 4$ between the exponents of about -0.45 ± 0.01 (100% volume content of polymer) and about -0.50 ± 0.01 (50% volume content of polymer) is mostly a result of the different chain statistics which is changing from a more Gaussian chain to a more self-avoiding walk with increasing degree of dilution. We find almost the same exponents for the systems with $f = 2$. The ratio for the prefactor of approximately $f - 1$ is in good agreement with the results from Leung and Eichinger.[13] This will be discussed below in more detail in conjunction with the rest of the data.

For the networks we can apply the same analysis as for the linear polymerizations concerning the dependence of cycles of different sizes on the extent of reaction. Figure 5 shows a plot analogous to Figure 3, but now for cycles of one, two, and three chains for the 10 independent systems with $N = 10$ at 50% volume content of polymer. For $p \leq 0.75$ we obtain for the functions $h_i(p) = a_i p^{2i}$ for rings of i-chains $a_1 = 0.0846 \pm 0.0004$, $a_2 = 0.0365 \pm 0.0003$, and $a_3 = 0.0343 \pm 0.0002$. All systems investigated show the same general trends, and again, the slowdown for the formation of rings of one chain at the very end of the simulation can be observed. However, for $p \leq 0.8$ and sometimes $p \leq 0.9$ we find very good agreement between $R_1^* p^2$ and $R_1(p)$ within all of our simulations. The data for all systems with $f = 4$ are summarized in Table 5. All our findings are now discussed and compared in the framework of previous simulations, experiments, and theories.

5. Discussion

The first issue shall be the discussion of rate theory as developed by Gordon and Temple[30] for the linear case. We can apply their results for the simple case of a random alternating linear (difunctional) copolymer directly, if we confine our analysis to connected pairs of chains and cross-links and take into account, that two reactions for ring formation are needed. The relative rate of formation dR_1/dR_2 was predicted to be proportional to $(E_1/E_2)2^{3/2}$ (cf. eq 4) when assuming a small number of rings. Concerning E_1 and E_2, we must keep in mind that our simulation is a stoichiometric alternating copolymerization reacting at random. Thus, we

Table 4. One-Chain Rings as a Function of the Network Chain Length[a]

	50% polymer		100% polymer	
	a	*b*	*a*	*b*
$f = 4$	$a = 0.238 \pm 0.003$	$b = -0.50 \pm 0.01$	$a = 0.142 \pm 0.006$	$b = -0.45 \pm 0.01$
$f = 2$	$a = 0.083 \pm 0.004$	$b = -0.46 \pm 0.02$	$a = 0.057 \pm 0.005$	$b = -0.42 \pm 0.03$

[a] The parameters for the functions $h(N) = aN^b$ used for the fitting of the number of one chain rings in Figure 4 are shown in this table. The data for $f = 2$ were obtained analogously for both volume contents of 50% and 100% of polymer.

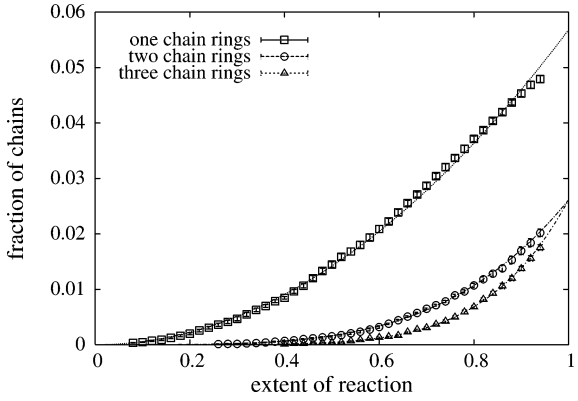

Figure 5. Number of one, two, and three chain rings in the innermost 50% of the systems displayed as a function of the extent of reaction. The averages over 10 independent networks with $N = 10$ and 100% volume content of polymer are shown.

Table 5. Rings of One, Two, and Three Chains in Networks with $f = 4$[a]

N	density	$a_1[10^{-4}]$	$a_2[10^{-4}]$	$a_3[10^{-4}]$	$a_1/2a_2$	$2a_2/3a_3$
10	50%	846 ± 4	365 ± 3	343 ± 3	1.16	0.71
22	50%	581 ± 2	258 ± 2	273 ± 3	1.13	0.63
43	50%	414 ± 1	199 ± 3	211 ± 2	1.04	0.63
82	50%	295 ± 3	159 ± 1	171 ± 1	0.93	0.62
153	50%	224 ± 2	95 ± 2	128 ± 1	1.18	0.50
10	100%	568 ± 2	261 ± 1	261 ± 1	1.09	0.67
22	100%	428 ± 3	224 ± 3	223 ± 3	0.96	0.67
43	100%	312 ± 2	157 ± 2	191 ± 4	0.99	0.55
82	100%	223 ± 1	124 ± 1	123 ± 1	0.90	0.67
153	100%	174 ± 1	72 ± 3	100 ± 2	1.21	0.48

[a] This table summarizes the parameters for the functions $h_i(p) = a_i p^{2i}$ with $i = 1, 2, 3$ used for the analysis of plots equivalent to Figure 5.

expect a number fraction of $2p(1-p)^2$ of pairs of one chain and one cross-link within the systems for E_1 and a fraction of $2p^3(1-p)^2$ for a sequence of two of these pairs E_2. Because of independent reactions, this leads to a relative rate of formation proportional to $2^{3/2}p^{-2} \approx 2.83p^{-2}$. We calculated this prefactor for p^{-2} using $h_i(p) = a_i p^{2i}$ as

$$\frac{\mathrm{d}h_1(p)}{\mathrm{d}h_2(p)}p^2 = \frac{a_1}{2a_2} \tag{17}$$

from the data. The last column of Table 3 presents the results in good agreement with the theoretical value of 2.83. Note that e.g. the value of 21 for a_2 corresponds to the small average number of 17 rings of two chains in the systems. This shows the reason why we had to restrict the analysis to $N \leq 43$. Thus, the data for $N = 10$ should show the highest accuracy.

Sarmoria et al.[49] obtain a similar behavior for the weight fractions of ring species (cf. Figure 2 of their work) in agreement with our results using the above theory. Since they show the weight fractions instead of the number fractions, the relative ratios differ accordingly. But we find a clear additional difference in Figures 3 and 5 that is increasing with conversion and is clearly leading to a higher total fraction of rings in our case than predicted by their approach. Their results are obtained by solving kinetic equations for different species of molecules. This stimulates additional simulations and theoretical investigations on kinetically driven systems using our approach.

Applying this analysis to the nonlinear polymerizations in Table 5, we have to consider that an *f*-functional cross-link allows for $f - 1$ possibilities of branching (cf. refs 3−5). Thus, we have to take the additional factor of $f - 1$ into account for each additional cross-link in a ring. For $f = 4$ this leads to

$$a_1/2a_2 = 2^{3/2}/(f-1) \approx 0.943 \tag{18}$$

and

$$2a_2/3a_3 = (3/2)^{3/2}/(f-1) \approx 0.612 \tag{19}$$

Comparing this with our data, we find a good agreement for this relative rates of ring formation, in particular when considering that chains, consumed in one chain rings, cannot form a linear assembly of two chains. The relative results for $2a_2/3a_3$ are not affected by the formation of one chain rings. Furthermore, the chain statistics changes for the systems at 50% polymer volume content. The analogy to the linear case indicates that we can use linear polymerizations to determine the length distribution and the amount of short cyclic material and we can transfer the results directly to the equivalent nonlinear reactions. The only difference is that we have to take the functionality of the molecules into account. However, we can use this findings to develop a general theory on ring formation within random polymerizations. To this end, we start with the simple case of linear homopolymerizations.

Selecting an unreacted group of a chain for reaction and assuming random reactions, the probability that the other end of this linear unit is *i* chains away is $p^{i-1}(1-p)$ since exactly $i - 1$ bonds are needed in between and the last reactive group is still able to react. Under this condition we know that the other end of the chain is always free. Thus, we can identify $c_{\mathrm{int},i} = c_{\mathrm{int}}{}^*\Phi(0,iN)$, or $c_{\mathrm{int},i} \sim i^{-3/2}$ when using Gaussian chain statistics. The concentration of the external material varies during the reaction as $c_{\mathrm{ext}} = c_{\mathrm{ext}0}(1-p)$. Using eq 5, we arrive at the rate

$$\frac{\mathrm{d}R_i}{\mathrm{d}p} = p^{i-1}(1-p)\frac{c_{\mathrm{int},i}}{c_{\mathrm{int},i} + c_{\mathrm{ext},0}(1-p)} \tag{20}$$

for ring formation. The right factor in this equation determines the probability for *i*-ring formation, and the left factor is the modified weight distribution of the linear species that can form cycles and a result of the reaction conditions. The present form of this equation corresponds to the undisturbed most probable weight distribution of a random reaction. A high weight fraction

of rings disturbs the weight distribution of the linear species in the irreversible case. Then, the weight distribution of the linear species has to be recalculated by considering the possible transitions between the molecular species. Note that our calculations are based on the extent of reaction for simplicity because the viscosity and thus the dynamics of the complete system change during the polymerization. This has to be taken into account when bringing forward our results to a dynamic analysis of ring formation.

Using the simplifying notation $c^* = c_{ext,0}/(c_{int}{}^*\Phi(0,iN))$, we find

$$R_i(p) = \frac{p^i(1 + c^* - iZ)}{(1 + c^*)ic^*} \tag{21}$$

with

$$Z = \sum_{n=0}^{\infty} \frac{[c^*p/(1 + c^*)]^n}{i + n} \tag{22}$$

This is the general solution for linear homopolymerizations with random reactions and a low weight fraction of rings or for linear ring−chain equilibria. For dense or semidilute systems of long linear monomers we have $c_{int} \ll c_{ext}$, and we can apply $c_{int,i} \sim i^{-3/2}$ as an approximation. Thus, eq 20 reduces to $dR_i/dp \sim p^{i-1}i^{-3/2}$ and leads to

$$R_i \sim p^i i^{-5/2} \tag{23}$$

Equation 20 can be generalized easily. For linear copolymerization the exponent for p changes from $i - 1$ to $2i - 1$, since we need i molecules for an i-chain ring of both types of molecules. For a copolymerization of an f-functional molecule of type A with a g-functional molecule of type B, we have to count the possibilities for branching for each molecule. Following branching theory,[3,4] the number of possibilities in eq 20 changes from p^{i-1} to $[p_A(f - 1)]^{i-1}[p_B(g - 1)]^i$ and the factors $(1 - p)$ change to $(1 - p_A)$ if a B group is selected for reaction. If an A group is selected, we have $[p_A(f - 1)]^i$-$[p_B(g - 1)]^{i-1}$ and $(1 - p_B)$. Replacing either p_A or p_B by use of the ratio of reactive groups on A and B molecules and integrating with respect to the remaining extent of reaction results in two equations for the formation of rings that depend on the type of the selected group. Applying these modifications, we find e.g. for the stoichiometric $p_A = p_B$ case with $c_{int} \ll c_{ext}$

$$R_i \sim i^{-5/2}[p_A(f - 1)p_B(g - 1)]^i \tag{24}$$

This special case is equivalent to the result of Suematsu in eq 15. However, eq 20 shows the principles of the general ansatz that can be used if not $c_{int} \ll c_{ext}$, if there are no stoichiometric conditions, and even if we have no random reactions. Additionally, eqs 20−24 show how rate theory is connected with the work of Suematsu. Note that eq 20 agrees well with the results of Tables 2, 3, and 5.

Leung and Eichinger[13,14] compare end-linked networks, which differ only in the number of chain monomers N and the functionality f of the cross-links. When comparing these systems, the density of reactive units is proportional to N^{-1} and the number of possibilities for branching for each cross-link is proportional to p_Ap_B-$(f - 1)$. Using eq 20 for random reactions and $c_{int,i} \sim N^{-3/2}$ for a comparison of the systems, we can estimate for the rings of one chain

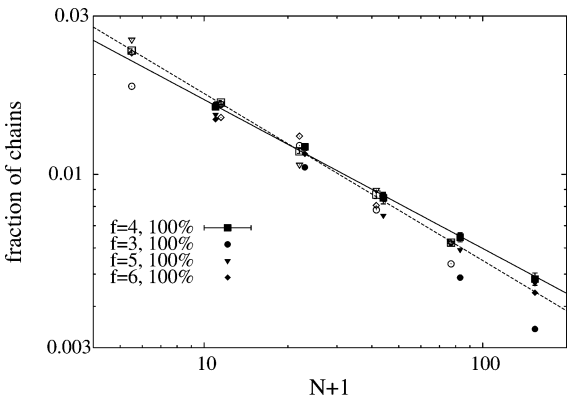

Figure 6. Unified plot for the one chain rings for the innermost 50% of networks with $f = 3, 4, 5, 6$. The x-axis is rescaled by the relative polymer density for the semidilute case and the y-axis by $1/(f - 1)$ as explained in the text. The full symbols show the results for the 100% polymer case and the hollow symbols for 50% polymers. The full line is the rescaled fitting function for dense $f = 4$ networks, the broken line displays the rescaled fit for the semidilute systems.

$$R_1(N) \sim p_Ap_B(f - 1)\frac{N^{-3/2}}{N^{-3/2} + c'N^{-1}} \tag{25}$$

with a modified constant c' that reflects the ratio of c_{ext} to c_{int} in the systems. If $c_{int} \ll c_{ext}$, it follows $c' \gg 1$ and in good approximation

$$R_1(N) \sim p_Ap_B(f - 1)N^{-1/2} \tag{26}$$

The dependence on $f - 1$ and $N^{-1/2}$ agrees well with the results of Leung and Eichinger[13,14] and the data in Table 4, in particular when taking the approximation $c' \gg 1$ and the changed chain statistics for the semidilute systems into account.

At this point we have to discuss the model functions $h_i(p) = a_ip^{2i}$ in section 4 for the fitting of the formation of i-chain rings. Since $c_{int} \ll c_{ext}$ for $p \leq 0.75$ and $p = p_A = p_B$ in our simulations, eq 24 shows ex post facto that we need no correction for the model functions in the range of $p \leq 0.75$. Additionally, eq 20 is able to explain the slowdown of the one chain ring formation at the very end of the reaction due to $p \to 1$.

Equation 26 shows that we can obtain a generalized plot for the one chain rings within all of our simulations for comparison. To this end we neglect the small changes in the chain statistics due to dilution. Then, the changes in the density of the reactive groups as a result of increasing chain length or dilution are comparable, and we can rescale the chain length for the diluted systems by multiplying with the change in polymer density. The effect of functionality is rescaled with dividing the number of one chain rings by $f - 1$. The result of this procedure is shown in Figure 6. Please note that the high scatter for the $f = 3$ case in Figure 6 is mostly due to the lower number of rings in these systems. Altogether we find a good consistency for the results of the different systems and no other clear trends when considering the above approximation and the small changes in chain statistics due to dilution.

Let us now compare our simulations with results from other groups. We will do this in approximation following the discussion of Binder[47] when the simulation methods

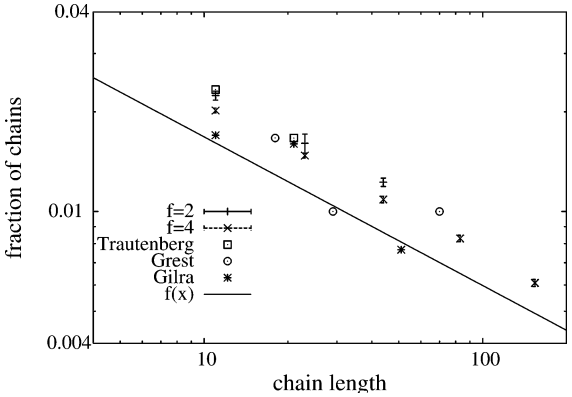

Figure 7. Unified plot of the fraction of one chain rings for the whole simulation container in the case of $f = 2$ and $f = 4$ in comparison with other simulations reported in the literature. The line is the rescaled fitting function for the innermost 50% of the dense $f = 4$ networks.

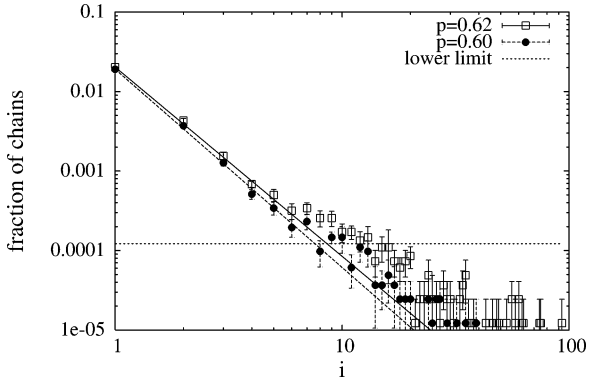

Figure 8. Distribution of i-rings at $p = 0.60$ and $p = 0.62$ averaged for 10 systems with 50% volume content of polymer and $N = 43$. The fitting was restricted to $i \leq 4$. The horizontal line indicates the inverse number of chains for the discussion of additional finite size effects.

are different. The discussed data for $f = 4$ are summarized in Figure 7. This figure includes both the fitted function for the innermost 50% and the data of the whole sample. In this way we estimate the effect of the borders and can compare simulations both with and without periodic boundary conditions. Note that the data in Figure 7 are rescaled by a factor of $1/(f - 1)$. Grest and Kremer[16] found for dense end-linked model networks with $f = 4$ and periodic boundaries a fraction of approximately 5% ($N = 12$) and 3% ($N = 25, 50$) single chain loops at almost full conversion. For comparison, the chain length of their work has to be multiplied by a factor of $\approx$1.3. Trautenberg et al.,[17] who used the same algorithm as this work with no periodic boundary conditions, found approximately 7% of one chain rings for dense systems with $N = 10$% and 5% for systems with $N = 20$. Gilra et al.[18] used the same simulation model as Trautenberg but periodic boundaries. They found approximately 5.1%, 4.8%, and 2.3% one chain rings for end-linked networks with chain lengths of $N = 10$, 20, and 50 monomers. Considering the different boundary conditions and the scatter in the data, we find good agreement between all simulations. In addition, we see that for comparable systems the effect of the borders concerning rings of one chain is about 20%. Except for this shift, we observe no systematic errors regarding the scaling of R_1 with N as a result of nonperiodic boundary conditions.

The final test of our work is summarized in Figure 8 displaying the ring distribution as a function of i close 10 systems with 50% volume content of polymer and $N = 43$. The ideal gel point p_c for four-functional end-linked networks is $p_c \approx 0.577$. When applying the theory of e.g. Suematsu,[40,41] we can estimate a gel point as a function of conversion and ring formation only. For all of our systems this estimated gel point is in the range of $0.59 < p_c < 0.63$; for the system of Figure 8 it is between both conversions displayed. For all systems of this study we fitted a function of type $h(i) = ai^b$ for $i < 5$ close to this estimated gel point in order to compare the data. We find results for the exponent in the range of -2.5 ± 0.1 for systems with 50% volume content of polymer and -2.35 ± 0.1 for 100% volume content of polymer. This agrees perfectly with our theory when considering the approximation $c_{ext} \gg c_{int}$ and the changed chain statistics for the systems with 50% volume content of polymer.

The lower limit in Figure 8 is determined by the inverse number of chains in our simulations. When the ring distribution reaches this line, an additional influence on the fraction of cycles due to the limited number of chains must occur. For $i < 7$ we find almost no influence, and for $i \geq 7$ there is a small influence. The increase of longer cyclic structures beyond the gel point at a conversion of $p = 0.62$ can be explained by a previous work[48] and is clearly influenced by the size of the simulation close to this critical point. However, we analyzed the shortest rings in the innermost 50% of the simulation box which are not influenced by the finiteness of the sample or the contacts with the border. In addition, we have to remark that the relation $R_1^* \sim N^{-1/2}$ leads to a small shift of the data points in Figure 8 for systems with longer chains. Thus, the relative influence of the finite size of the sample and the additional intramolecular reactions increase with chain length for systems with the same number of chains but are still not affected by the finite size of the system, when restricting the analysis to the innermost 50% of the sample.

6. Summary

Using computer simulations, we investigated intramolecular reactions in irreversible polymerizations. Since for our simulations the reactions take place at random, we can use our results to investigate randomly reacting systems and ring chain equilibria. We find that the relative rate for ring formation is proportional to $i^{-3/2}$, in agreement with rate theory. Using a modified ansatz of Stepto, the laws of conditional probability, and rate theory, we find a general equation for the ring formation. Using the approximation $c_{ext} \gg c_{int}$, this ansatz reduces to the result of Suematsu.[40,41] With this general equation we are able to explain the results on ring formation of preceding simulations[16−18] and this work. Since our work generalizes and combines existing theories on ring formation, the good agreement of this theoretical work with experiments additionally approves our results. In the case of $c_{ext} \gg c_{int}$ we find for the ring size distribution R_i at the gel point $R_i \sim i^{-5/2}$, and in general $R_i \sim i^{-5/2}[(f - 1)(g - 1)p_A p_B]^{i-1}$. For small $i = 1$, 2, 3 this relation is valid up to full conversion in good approximation. When comparing systems, which differ only in the length of the chains, the change in ring formation is proportional to $N^{-1/2}$. A comparison with kinetically driven calculations[49] shows some differences

to the present work and will be the topic of a forthcoming study as well as the application of our results to the theory on polymer networks.

Acknowledgment. Michael Lang thanks the Deutsche Forschungsgemeinschaft (Kr1272/6-1) and the Universität Regensburg for financial support and the facilities of the Universität Regensburg and the Leibniz Rechenzentrum München for a generous grant of computing time.

References and Notes

(1) Stockmayer, W. H. *J. Chem. Phys.* **1943**, *11*, 45−55.
(2) Stockmayer, W. H. *J. Chem. Phys.* **1944**, *12*, 125−131.
(3) Flory, P. J. *Principles of Polymer Chemistry*; Cornell University Press: Ithaca, NY, 1953.
(4) Macosko, C. W.; Miller, D. R. *Macromolecules* **1976**, *9*, 199−206.
(5) Miller, D. R.; Macosko, C. W. *Macromolecules* **1976**, *9*, 206−211.
(6) Tonelli, A. E.; Helfand, E. *Macromolecules* **1974**, *7*, 59−63.
(7) Helfand, E.; Tonelli, A. E. *Macromolecules* **1974**, *7*, 832−834.
(8) Dusek, K.; Gordon, K.; Ross-Murphy, S. B. *Macromolecules* **1978**, *11*, 236−245.
(9) Dusek, K. In *Developements in Polymerisation−3*; Haward, R. N., Ed.; Applied Science Publishers: London,1982; pp 143−206.
(10) Lang, M.; Göritz, D.; Kreitmeier, S. *Macromolecules* **2003**, *36*, 4646−4658.
(11) Shy, L. Y.; Eichinger, B. E. *Macromolecules* **1986**, *19*, 2787−2793.
(12) Grest, G. S.; Kremer, K. *Macromolecules* **1990**, *23*, 4994−5000.
(13) Leung, Y.-K.; Eichinger, B. E. *J. Chem. Phys.* **1984**, *80*, 3877−3884.
(14) Leung, Y.-K.; Eichinger, B. E. *J. Chem. Phys.* **1984**, *80*, 3885−3891.
(15) Lee, K. J.; Eichinger, B. E. *Macromolecules* **1988**, *22*, 1441−1448.
(16) Grest, G. S.; Kremer, K.; Duering, E. R. *Eur. Phys. Lett.* **1992**, *19*, 195−200.
(17) Trautenberg, H. L.; Sommer, J. U.; Göritz, D. *Macromol. Symp.* **1994**, *81*, 153−160.
(18) Gilra, N.; Cohen, C. *J. Chem. Phys.* **2001**, *112*, 6910−6916.
(19) Erman, B.; Mark, J. E. *Structure and Properties of Rubberlike Networks;* Oxford University Press: New York, Oxford, 1997.
(20) Llorente, M. A.; Mark, J. E. *J. Chem. Phys.* **1979**, *71*, 682−689.
(21) Ahmad, Z.; Stepto, R. F. T. *Colloid Polym. Sci.* **1980**, *258*, 663−674.
(22) Rolfes, H.; Stepto, R. F. T. *Makromol. Chem. Macromol. Symp.* **1993**, *76*, 1−12.
(23) Gottlieb, M.; Macosko, C. W.; Benajamin, G. S.; Meyers, K. O.; Merill, E. W. *Macromolecules* **1981**, *14*, 1039−1046.
(24) Patel, S. K.; Malone, S.; Cohen, C.; Gillmor, J. R.; Colby, R. H. *Macromolecules* **1992**, *25*, 5241−5251.
(25) Hild, G. *Prog. Polym. Sci.* **1998**, *23*, 1019−1149.
(26) Jacobson, H.; Stockmayer, W. H. *J. Chem. Phys.* **1950**, *18*, 1600−1606.
(27) Kloczkowski, A.; Jernigan, R. L. *Comput. Theor. Polym. Sci.* **1999**, *9*, 285−294.
(28) Flory, P. J.; Semlyen, J. A. *J. Am. Chem. Soc.* **1966**, *88*, 3209−3212.
(29) Flory, P. J.; Suter, U.; Mutter, M. J. *J. Am. Chem. Soc.* **1976**, *98*, 5733−5739.
(30) Gordon, M.; Temple, W. B. *Makomol. Chem.* **1972**, *160*, 263−276.
(31) Stanford, J. L.; Stepto, R. F. T. *J. Chem. Soc., Faraday Trans. 1* **1974**,*71*, 1292−1307.
(32) Stanford, J. L.; Stepto, R. F. T.; Waywell, D. R. *J. Chem. Soc., Faraday Trans. 1* **1974**, *71*, 1308−1326.
(33) Kuhn, W.; Grühn, F. *J. Polym. Sci.* **1946**, *1*, 183−199.
(34) Semlyen, J. A. In *Cyclic Polymers*; Semlyen, J. A., Ed.; Elsevier: London, 1986; pp 1−41.
(35) Winnik, M. A. In *Cyclic Polymers*; Semlyen, J. A., Ed.; Elsevier: London, 1986; pp 285−348.
(36) Stepto, R. F. T. In *Developements in Polymerisation−3*; Haward, R. N., Ed.; Applied Science Publishers: London, 1982; pp 81−141.
(37) Stepto, R. F. T.; Taylor, D. J. R. *Polym. Gels Networks* **1996**, *4*, 405−414.
(38) Stepto, R. F. T. In *Polymer Networks*; Stepto, R. F. T., Ed.; Blackie Academic and Professional: London, 1998; pp 15−63.
(39) Kilb, R. W. *J. Phys. Chem.* **1958**, *62*, 969−971.
(40) Suematsu, K. *Eur. Phys. J. B* **1998**, *6*, 93−100.
(41) Suematsu, K. *Adv. Polym. Sci.* **2002**, *156*, 137−214.
(42) Carmesin, I.; Kremer, K. *Macromolecules* **1988**, *21*, 2819−2823.
(43) Michalke, W.; Lang, M.; Kreitmeier, S.; Göritz, D. *J. Chem. Phys.* **2002**, *117*, 6300−6307.
(44) Hölzl, T.; Trautenberg, H. L.; Göritz, D. *Phys. Rev. Lett.* **1997**, *79*, 2293−2296.
(45) Michalke, W.; Lang, M.; Kreitmeier, S.; Göritz, D. *Phys. Rev. E* **2001**, *64*, 012801.
(46) Lang, M.; Göritz, D.; Kreitmeier, S. In *Constitutive Models for Rubber III*; Busfield, J. J. C., Muhr, A. H., Eds.; Swets & Zeitlinger: Lisse, The Netherlands, 2003; pp 195−202.
(47) Binder, K. In *Monte Carlo and Molecular Dynamics Simulations in Polymer Science*; Binder, K., Ed.; Oxford University Press: Oxford, 1995; pp 3−46.
(48) Lang, M.; Michalke, W.; Kreitmeier, S. *J. Chem. Phys.* **2001**, *114*, 7627−7632.
(49) Sarmoria, C.; Valles, E.; Miller, D. R. *Macromol. Chem., Macromol. Symp.* **1986**, *2*, 69−87.
(50) Lang, M.; Michalke, W.; Kreitmeier, S. *Macromol. Theory Simul.* **2001**, *10*, 204−208.

MA049025Z